ACS APPLIED ENERGY MATERIALS

www.acsaem.org Letter

Argyrodite Superionic Conductors Fabricated from Metathesis-Derived Li_2S

William H. Smith, Saeed Ahmadi Vaselabadi, and Colin A. Wolden*

Cite This: https://doi.org/10.1021/acsaem.2c00442 Read Online

ACCESS | Metrics & More | Article Recommendations | Supporting Information

ABSTRACT: Lithium sulfide (Li_2S) is both a high-capacity cathode and the critical component in sulfide-based lithium-ion solid-state electrolytes. Conventionally produced by carbothermal or H_2S reduction, its high cost constrains development of the next-generation batteries that employ it. Here, we introduce production of Li_2S though room-temperature (RT) metathesis using LiCl and technical grade $Na_2S{\cdot}xH_2O$ that was either dehydrated or further purified through hydrogen reduction. Li_6PS_5Cl argyrodites derived from metathesis Li_2S display high ionic conductivity (>4 mS cm^{-1} at RT), exceeding that of the commercial Li_2S control. Metathesis offers an economical and energy efficient route for the scalable production of this critical material.

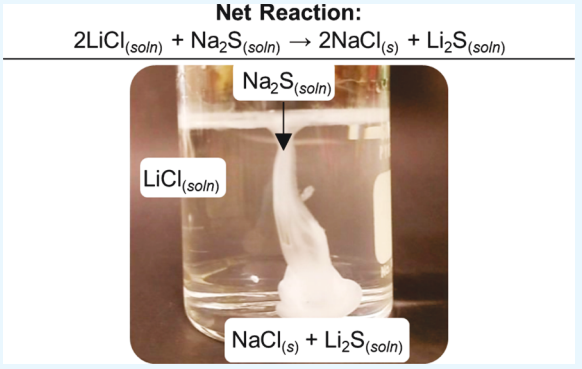

KEYWORDS: *lithium sulfide, argyrodite, solid electrolyte, metathesis, ionic conductivity*

Conventional lithium-ion batteries (LIBs) used in today's electric vehicles (EVs) are approaching their physico-chemical limit for energy density, which is constraining their wider adoption due to both range and cost considerations.[1] Replacement of conventional liquid electrolytes with thin solid-state counterparts is key to enhancing the specific energy density of next-generation batteries while simultaneously reducing flammability concerns.[2] All-solid-state lithium-ion batteries (ASSLIBs) could employ conventional electrodes (graphite/metal oxides) or be paired with anodes (Li, Si)[3,4] or cathodes (S, Li_2S)[5] that offer higher capacity.

Candidate SSEs include polymers, oxides, and sulfide-based inorganic glasses and ceramics. Among these, the latter offer favorable properties including superior ionic conductivity[6] and ductility, which allows for the effective formation of electrolyte−electrode interfaces.[2] Among the most promising sulfide SSEs are the Li_2S−P_2S_5 (LPS) glasses and ceramics (i.e., $Li_7P_3S_{11}$), $Li_{10}GeP_2S_{12}$ (LGPS) and its analogues, and $Li_{7-y}PS_{6-y}X_y$ (X = Cl, Br, I) argyrodites.[7] Chloride argyrodites (Li_6PS_5Cl) in particular are favored due to their combination of high ionic conductivity ($\sigma_{25\,^\circ C} \approx 1-5$ mS cm^{-1}),[8] favorable synthesis and processing methods,[9] lack of expensive materials such as GeS_2, and the self-passivating nature of its interfaces.[10]

However, a major disadvantage of sulfide SSEs is their high cost, which is primarily due to the high cost of the key precursor lithium sulfide (Li_2S). Laboratory quantities of Li_2S retail for > $10,000/kg, and at scale the price remains ~$1,000/kg, which is not competitive with current LIB technology. The high cost of Li_2S reflects the unfavorable methods used to synthesize it, summarized in Table 1. Lithium metal can be reacted with elemental sulfur or H_2S. As recently reported, the elemental reaction can be conducted at ~90 °C in tetrahydrofuran (THF) with an electron transfer catalyst such as naphthalene.[11] Alternatively, lithium can be converted to an intermediate alkoxide solution and then reacted with H_2S gas at ambient temperatures.[12−15] Fast kinetics coupled with favorable thermodynamics ensure complete abatement of the hazardous waste gas and concomitant recovery of the H_2 contained therein. These methods may be preferred at laboratory scale due to their simplicity, but large-scale production is unfavorable due to the high cost of lithium metal relative to more common lithium salts. Furthermore, this process required purified H_2S and presents toxicity and flammability hazards, as does lithium metal due to its pyrophoricity and THF due to its toxicity. The industrial standard is the carbothermal reduction of lithium sulfate due to the low cost of reagents and technological maturity, but this method requires higher operating costs due to the highly endothermic nature of the reaction, which is typically conducted around 700−1,000 °C.[16] Due to the energy intensity and reaction stoichiometry, carbothermal reduction is the most CO_2-intensive synthesis route. Li_2CO_3 and LiOH

Received: February 9, 2022
Accepted: March 29, 2022

Table 1. Attributes of the Alternative Li_2S Synthesis Methods

Lithium Source	Cost[a] (USD kg^{-1} Li)	Reaction	Process Temp[b] (°C)	Energy[c] (MJ kg^{-1} Li_2S)	GHG[d] (kg CO_2 kg^{-1} Li_2S)	Safety/ Hazards
Li	73.0	$2Li + S \xrightarrow{THF} Li_2S$	90	11.6	0.59	Li, THF
		$2Li + H_2S \xrightarrow{EtOH} Li_2S + H_2$	20/300	39.0	1.96	Li, H_2S
Li_2SO_4	31.0	$Li_2SO_4 + 2C \xrightarrow{\Delta} Li_2S + 2CO_2$	700-1000/300	27.3	3.29	Hi T
Li_2CO_3	26.9	$Li_2CO_3 + H_2S \xrightarrow{\Delta} Li_2S + CO_2 + H_2O$	500-700	5.1	1.22	H_2S/Hi T H_2S/H_2O
LiOH	43.7	$2LiOH + H_2S \xrightarrow{\Delta} Li_2S + H_2O$	250-450	5.0	0.25	H_2S/Hi T H_2S/H_2O
LiCl	52.5	$2LiCl + Na_2S \xrightarrow{EtOH} Li_2S + 2NaCl$	20/300	22.2	1.11	N/A

[a]References 16, 20, and 21. [b]Reaction/annealing (if needed). [c]Includes precursor formation (electrolysis, dehydration)/reaction/solvent evaporation (if needed). See Tables S1−S6 for a detailed summary. [d]Direct CO_2 evolution + 0.05 kg of CO_2 MJ^{-1} (carbon intensity of natural gas).

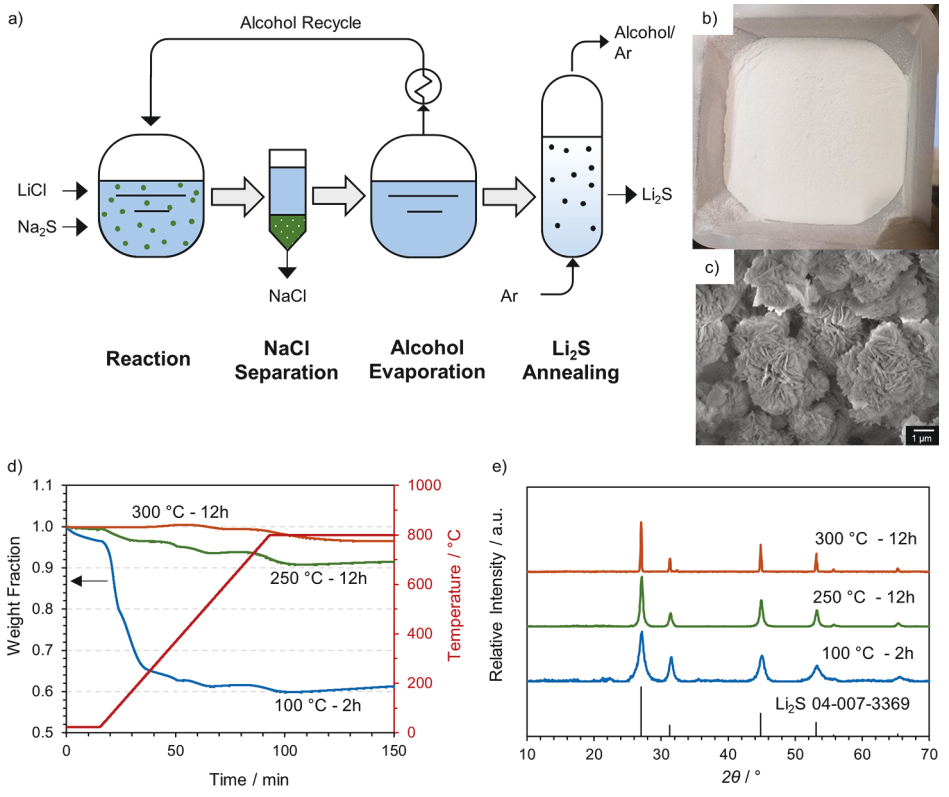

Figure 1. (a) Process flow diagram of the low-temperature liquid-state metathesis for the production of Li_2S. (b) Image and (c) micrograph of metathesis Li_2S. (d) TGA and (e) XRD of Li_2S after sequential thermal processing steps.

may also be reduced with H_2S at elevated temperatures.[17,18] Drawbacks of these approaches, however, are relatively slow solid−gas reaction kinetics and the highly corrosive nature of the resulting mixtures of unreacted H_2S and steam. These high-temperature methods also produce Li_2S in bulk form, often requiring additional purification and processing such as ball milling to deliver powders with the desired morphology. An alternative approach employs alcohol extraction and subsequent distillation/annealing.[19]

A common reaction method for synthesizing transition metal sulfides is the metathesis—or counterion exchange—reaction, but the application of this method to the synthesis of Li_2S has not yet been reported in the literature. Here, we describe the development of a reaction scheme in which lithium chloride reacts with Na_2S in an alcohol solution. Reactive precipitation of NaCl provides favorable energetics and facilitates separation of the two products due to the high solubility of Li_2S in alcohols relative to NaCl. The Li_2S is

https://doi.org/10.1021/acsaem.2c00442
ACS Appl. Energy Mater. XXXX, XXX, XXX−XXX

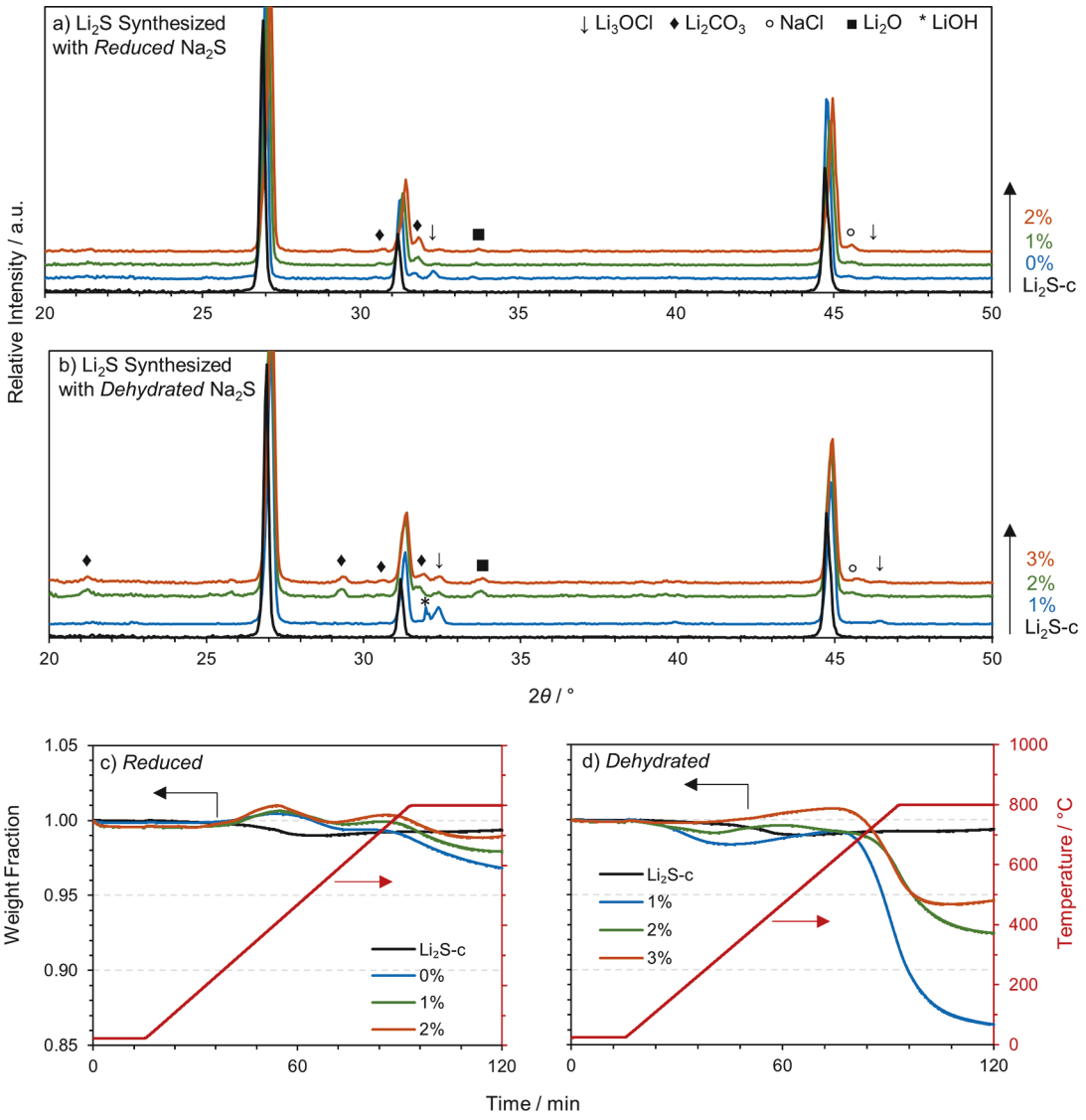

Figure 2. (a, b) XRD and (c, d) TGA of Li_2S derived from H_2-reduced and dehydrated Na_2S, respectively, along with a commercial Li_2S sample.

recovered via solvent evaporation and purified by annealing at 300 °C under flowing argon. Panels a and b of Figure 1 provide a flow diagram of the metathesis process and image of the final Li_2S product, respectively.

Anhydrous Na_2S, like its lithium counterpart, is currently prohibitively expensive. Instead we employ low-cost, technical grade Na_2S hydrate flakes (~$0.5/kg at scale) that are purified in house using a two-step procedure detailed previously.[22] A low-temperature anneal removes bound water and a hydrogen reduction step removes residual polysulfide and oxysulfur impurities, resulting in anhydrous Na_2S powders with purity superior to that of commercially available material. Both dehydrated and fully reduced Na_2S were used and compared. The metathesis reaction was conducted by adding a near-stoichiometric quantity of purified Na_2S reagent directly to an LiCl solution with stirring. Upon addition of Na_2S a white suspension rapidly forms due to NaCl precipitation. Next, the NaCl solids are separated out by centrifugation, and the supernatant is evaporated under vacuum with stirring at 100 °C. Additional details on the process conditions and representative images (Figure S1) are provided in the Supporting Information.

The powder recovered from the evaporation step appears dry but retains 40 wt % solvent (Figure 1d), necessitating further annealing at elevated temperatures above 200 °C to completely remove complexed solvent. Annealing above 300 °C or in the presence of strong mass transfer limitations can cause carburization of solvent resulting in a gray discoloration to the Li_2S, identified as carbon deposits by observation of carbon D/G bands in Raman spectroscopy. (Figure S2) Therefore, the Li_2S samples were annealed in a fluidized-bed configuration (Figure S7) to minimize transport limitations, and the annealing temperature was limited to 300 °C or below. TGA (Figure 1d) shows that a 250 °C anneal for 12 h reduces the solvent content to ~4 wt %, and a further anneal at 300 °C for 12 h is required to completely remove the solvent. Solvent removal throughout annealing is accompanied by an increase in crystallite size as evidenced by the peak broadening exhibited in XRD (Figure 1e). A Scherrer equation estimate indicates crystallites smaller than 10 nm in the as-evaporated material and ~18 nm in the 250 °C annealed material, while the 300 °C annealed material exhibits sharp diffraction peaks consistent with much larger particle sizes. These nanocrystals can be observed in SEM as consisting of nanoflakes with

https://doi.org/10.1021/acsaem.2c00442
ACS Appl. Energy Mater. XXXX, XXX, XXX−XXX

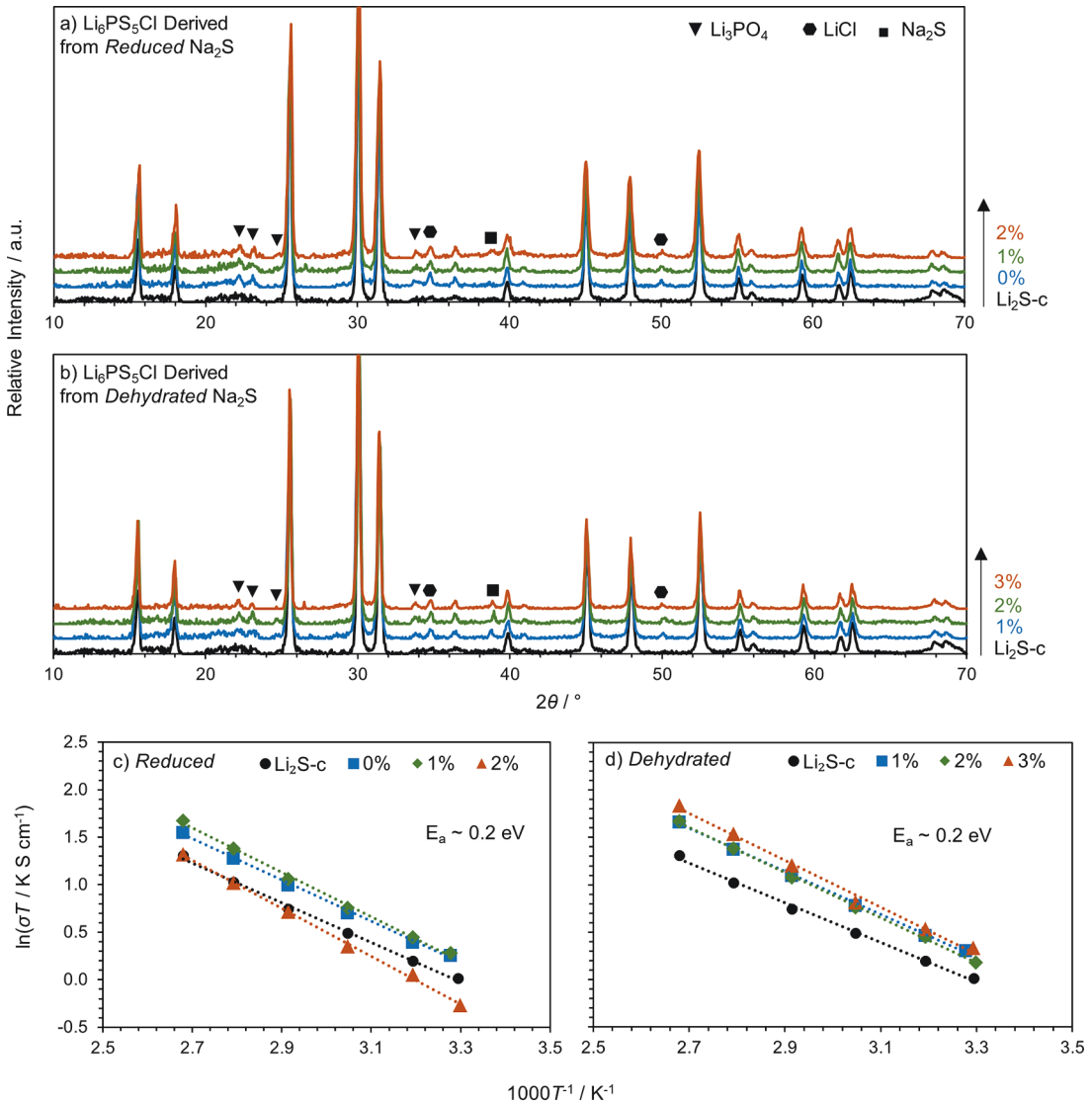

Figure 3. (a, b) XRD and (c, d) Arrhenius plots of ionic conductivity for argyrodites synthesized with Li_2S derived from high-purity and low-purity Na_2S, respectively, along with an argyrodite synthesized from a commercial Li_2S sample.

thicknesses on the order of 100 nm, which agglomerate into spherical secondary particles about 1−10 μm in diameter (Figure 1c and Figure S3). In previous work, we demonstrated that this nanoflake morphology is beneficial for applications both to Li_2S cathodes[14] and in the mechanochemical synthesis of glassy solid-state electrolytes.[15]

The Li_2S recovered from metathesis is of high purity, but residual impurities not present in commercial material were detected with XRD and TGA. Figure 2 compares the properties of metathesis Li_2S relative to a commercial standard as a function of Na_2S source (dehydrated or fully reduced) and the Na_2S:LiCl stoichiometry. Using fully reduced Na_2S XRD revealed the presence of several impurity phases, Li_3OCl, Li_2O, and Li_2CO_3, and NaCl. Conducting the same synthesis with a slight stoichiometric excess Na_2S (1 or 2 wt %) diminished the intensity of the Li_3OCl diffraction peak, while the relative intensity of the Li_2CO_3 and NaCl peaks increased (Figure 2a) This may suggest that the presence of impurities in the Na_2S reagent necessitates an additional excess above the nominal stoichiometry in order to completely consume all of the LiCl reagent. Otherwise, the unreacted LiCl may react with oxygenated lithium compounds to form Li_3OCl. We presume that O and C impurities derive from the decomposition of the solvated compound $Li_2S{\cdot}CH_3CH_2OH$ that is present in Li_2S recovered from ethanol solutions.[23] Optimization of annealing conditions minimized but failed to completely eliminate these impurities.

TGA can provide semiquantitative information about concentrations of LiOH and Li_2CO_3, which decompose to Li_2O and H_2O at around 600 °C and Li_2O and CO_2 at around 800 °C, respectively.[24] For example, the commercial sample exhibits an ∼1 wt % mass loss around 600 °C, suggesting LiOH impurities present on the order of 2.5 wt %, though no LiOH is detected in XRD. The commercial sample is stable at 800 °C, suggesting the absence of Li_2CO_3, while the synthesized samples display a significant mass loss at 800 °C that decreases linearly with Na_2S excess. (Figure 2c) However, this trend is opposite that observed in XRD, suggesting that the mass loss at 800 °C may be attributed to additional impurities. The decreasing Li_3OCl content exhibited in XRD suggests that the mass loss may instead be due to thermal

https://doi.org/10.1021/acsaem.2c00442
ACS Appl. Energy Mater. XXXX, XXX, XXX−XXX

decomposition of Li_3OCl to Li_2O and LiCl followed by subsequent LiCl volatilization.

The precipitate was predominantly NaCl by XRD in all cases. However, FTIR spectroscopy revealed the presence of trace quantities of Na_2SO_x impurities (Figure S4). It is suggested that the Na_2SO_x species are derived from the Na_2S reagent and act as spectators in the metathesis reaction due to their low solubility in EtOH, therefore passing into the precipitate unreacted. This is consistent with the notion that excess Na_2S is required to fully consume the LiCl precursor due to the presence of such inert impurities. Because of this finding, it was hypothesized that anhydrous Na_2S could be used without purification via H_2 reduction and would simply require a slightly greater excess to account for the higher concentration of Na_2SO_x in the dehydrated material. Aside from Na_2SO_x impurities, the dehydrated Na_2S used in this study also contains sodium polysulfides, which are soluble in EtOH, and presumably participates in the metathesis reaction similar to Na_2S. The reaction supernatant resulting from its use is bright yellow in contrast to the colorless solution obtained when H_2-reduced Na_2S is employed (Figure S5). The as-dried Li_2S retains a light-yellow color, suggesting the presence of polysulfide species.[25] However, annealing at 250 °C converts the material's color to white, suggesting thermal decomposition of the polysulfides.

Figure 2b shows XRD of Li_2S samples prepared from dehydrated Na_2S without H_2 reduction. Li_2S synthesized from a 1 wt % excess of dehydrated Na_2S exhibits diffraction peaks attributed to Li_3OCl and NaCl along with an unidentifiable compound with a diffraction peak at ∼32.0°. In TGA (Figure 2d) this same sample, as well as a sample synthesized from 2 wt % excess, exhibits an anomalous mass loss with an onset around 200 °C, which does not correspond to any of the previously identified impurities. Li_2S samples synthesized from excesses of dehydrated Na_2S exhibit the same trends as samples synthesized from H_2-reduced Na_2S: the relative intensity of the Li_3OCl diffraction peaks decreased with increasing Na_2S excess, and the TGA mass loss at 800 °C decreased monotonically, while the relative intensity of Li_2CO_3 diffraction peaks increased. The greater mass loss exhibited by samples derived from dehydrated Na_2S without purification may suggest the retention of Na_2SO_x or Na_2S_x species, which may decompose to Na_2S and small gas molecules at high temperatures.

To investigate the validity of metathesis synthesized Li_2S, the samples were subsequently employed in the synthesis of Li_6PS_5Cl argyrodite solid-state electrolytes. Stoichiometric quantities of Li_2S, P_2S_5, and LiCl were ball-milled and then annealed at 550 °C to produce crystalline Li_6PS_5Cl. Figure 3 compares the structure and performance of argyrodite electrolytes derived from metathesis Li_2S relative to a commercial standard again as a function of Na_2S source and stoichiometry. Li_6PS_5Cl synthesized from the commercial sample of Li_2S exhibits X-ray diffraction peaks that can only be attributed to the argyrodite phase with no impurities or unreacted precursors detected. The Li_6PS_5Cl samples prepared from metathesis Li_2S display a number of impurity phases. All samples, regardless of Na_2S purification, exhibit Li_3PO_4 and LiCl impurities, presumably originating in oxygenated and chlorinated species such as Li_2CO_3, Li_2O, and Li_3OCl present in the synthesized Li_2S. In the samples derived from dehydrated Na_2S (and in the sample prepared from 2 wt % excess H_2-reduced Na_2S) residual Na_2S is detected. In the sample prepared from H_2-reduced Na_2S, this may simply suggest that 2 wt % excess results in unreacted Na_2S that remains dissolved in the supernatant fraction. In contrast, when dehydrated Na_2S is used, Na_2S is present even when Li_3OCl levels were high—indicating a substoichiometric quantity of Na_2S—which suggests that the Na_2S is instead derived from impurities in the Na_2S, which apparently can partition into the final Li_2S product. These impurities, such as Na_2SO_x and Na_2S_x, may then decompose into Na_2S during Li_6PS_5Cl synthesis and processing (Figure 3a,b).

While phase purity is important, performance is paramount, and therefore the ionic conductivity of the argyrodites was measured by temperature-dependent electrochemical impedance spectroscopy. The room-temperature ionic conductivity of the sample prepared from commercial Li_2S was 3.34 mS cm^{-1} with an activation energy of 0.18 eV. The literature value for the activation energy of Li_6PS_5Cl is reported as either ∼0.35 or ∼0.2 eV.[26] The cause of this discrepancy is currently not fully understood but has been attributed to variations in chemical purity[27] or variations in Cl^-/S^{2-} distribution in the $Li_{7-x}PS_{6-x}Cl_x$.[28] Importantly, despite the presence of trace impurities, all of the metathesis-based argyrodites displayed nominally identical performance to the commercial baseline. Room-temperature ionic conductivities ranged from 2.52 to 4.21 mS cm^{-1} and activation energies equal to 0.2 ± 0.02 eV (Figure 3c,d). Room-temperature Nyquist plots are presented in Figure S6, and values for ionic conductivity and activation energy are tabulated in Table S7. Most of these samples exceed all previously reported conductivity values for the Li_6PS_5Cl[8] with the exception of one report that employed extreme fabrication pressure (1000 MPa/4.96 mS cm^{-1}).[29] While ionic conductivity is the primary figure of merit for these materials, the electronic conductivity is also key for maintaining low leakage current and suppressing lithium dendrite growth.[30] DC polarization experiments found electronic conductivity ranging from 1×10^{-6} to 3×10^{-6} mS cm^{-1}, in good comparison with the literature.[31]

The current cost of Li_2S is a bottleneck to widespread deployment of solid-state batteries employing sulfide-based electrolytes. Table 1 compares the attributes of metathesis production of Li_2S with the alternatives employed to date. None of the current synthesis approaches successfully balances low materials costs with low-intensity processing and nonhazardous conditions. Metathesis is an exceptionally benign process that provides a compelling alternative with no outstanding drawbacks. LiCl is a moderate cost precursor, and there is potential for its price to decrease because up to 80% of the world's lithium reserves are in brines[32] and there is substantial ongoing work to improve recovery technologies.[33] Even at current pricing, the materials cost for metathesis is < \$50 kg^{-1} Li_2S due to the negligible cost of Na_2S and recycling of the ethanol. The modest energy and GHG emissions are primarily associated with ethanol vaporization. Alternatively dissolved Li_2S could be used directly in solution-based electrolyte synthesis methods that are being developed as more scalable alternatives to ball milling.[34] The leading attributes of metathesis are its low temperature, fast kinetics, absence of safety concerns, and generation of powders with favorable morphology for subsequent processing.

In summary, this study demonstrates solution-based synthesis of Li_2S via metathesis conducted in ethanol using low-cost precursors LiCl and $Na_2S{\cdot}xH_2O$. Li_2S powders were recovered via solvent evaporation followed by a mild anneal at

https://doi.org/10.1021/acsaem.2c00442
ACS Appl. Energy Mater. XXXX, XXX, XXX−XXX

300 °C. Metathesis Li_2S retained residual impurities not observed in commercial Li_2S that originate from the reagents employed and ethanol decomposition during annealing. Nevertheless, Li_6PS_5Cl argyrodite electrolytes synthesized from metathesis Li_2S demonstrated a combination of properties including high room-temperature ionic conductivity (3−4 mS cm^{-1}), low electronic conductivity (~10^{-6} mS cm^{-1}), and low activation energy (~0.2 eV) that were comparable to the commercial control and among the best achieved to date for this material. The combination of low precursor costs coupled with fast and benign processing offers the opportunity to reduce Li_2S costs more than an order of magnitude, making solid-state batteries technologies employing thio-LISICON electrolytes cost competitive. Work is ongoing to further improve the Li_2S impurity profile and assess its impact in other applications such as advanced cathodes.

■ ASSOCIATED CONTENT

Supporting Information

The Supporting Information is available free of charge at https://pubs.acs.org/doi/10.1021/acsaem.2c00442.

Experimental methods, additional material characterization, Nyquist plots, ionic conductivity and activation energy summary, and Supporting Information for Table 1 (PDF)

■ AUTHOR INFORMATION

Corresponding Author

Colin A. Wolden − *Chemical and Biological Engineering, Colorado School of Mines, Golden, Colorado 80401, United States*; orcid.org/0000-0001-6576-048X; Email: cwolden@mines.edu

Authors

William H. Smith − *Chemical and Biological Engineering, Colorado School of Mines, Golden, Colorado 80401, United States*

Saeed Ahmadi Vaselabadi − *Chemical and Biological Engineering, Colorado School of Mines, Golden, Colorado 80401, United States*

Complete contact information is available at: https://pubs.acs.org/10.1021/acsaem.2c00442

Notes

The authors declare no competing financial interest.

■ ACKNOWLEDGMENTS

This work was supported by the National Science Foundation through Award 1825470, the Colorado Office of Economic Development and International Trade, and Solid Power.

■ REFERENCES

(1) Masias, A.; Marcicki, J.; Paxton, W. A. Opportunities and Challenges of Lithium Ion Batteries in Automotive Applications. *ACS Energy Lett.* **2021**, *6*, 621−630.

(2) Wu, J.; Liu, S.; Han, F.; Yao, X.; Wang, C. Lithium/Sulfide All-Solid-State Batteries using Sulfide Electrolytes. *Adv. Mater.* **2021**, *33* (6), 2000751.

(3) Lee, Y.-G.; Fujiki, S.; Jung, C.; Suzuki, N.; Yashiro, N.; Omoda, R.; Ko, D.-S.; Shiratsuchi, T.; Sugimoto, T.; Ryu, S.; Ku, J. H.; Watanabe, T.; Park, Y.; Aihara, Y.; Im, D.; Han, I. T. High-energy long-cycling all-solid-state lithium metal batteries enabled by silver−carbon composite anodes. *Nat. Energy* **2020**, *5*, 299.

(4) Tan, D. H. S.; Chen, Y.-T.; Yang, H.; Bao, W.; Sreenarayanan, B.; Doux, J.-M.; Li, W.; Lu, B.; Ham, S.-Y.; Sayahpour, B.; Scharf, J.; Wu, E. A.; Deysher, G.; Han, H. E.; Hah, H. J.; Jeong, H.; Lee, J. B.; Chen, Z.; Meng, Y. S. Carbon-free high-loading silicon anodes enabled by sulfide solid electrolytes. *Science* **2021**, *373*, 1494−1499.

(5) Wu, F.; Kim, H.; Magasinski, A.; Lee, J. T.; Lin, H.-T.; Yushin, G. Harnessing Steric Separation of Freshly Nucleated Li2S Nanoparticles for Bottom-Up Assembly of High-Performance Cathodes for Lithium-Sulfur and Lithium-Ion Batteries. *Adv. Energy Mater.* **2014**, *4* (11), 1400196.

(6) Bachman, J. C.; Muy, S.; Grimaud, A.; Chang, H. H.; Pour, N.; Lux, S. F.; Paschos, O.; Maglia, F.; Lupart, S.; Lamp, P.; Giordano, L.; Shao-Horn, Y. Inorganic Solid-State Electrolytes for Lithium Batteries: Mechanisms and Properties Governing Ion Conduction. *Chem. Rev.* **2016**, *116* (1), 140−62.

(7) Deiseroth, H. J.; Kong, S. T.; Eckert, H.; Vannahme, J.; Reiner, C.; Zaiss, T.; Schlosser, M. Li6PS5X: a class of crystalline Li-rich solids with an unusually high Li+ mobility. *Angew. Chem., Int. Ed. Engl.* **2008**, *47* (4), 755−8.

(8) Doux, J.-M.; Yang, Y.; Tan, D. H. S.; Nguyen, H.; Wu, E. A.; Wang, X.; Banerjee, A.; Meng, Y. S. Pressure effects on sulfide electrolytes for all solid-state batteries. *J. Mater. Chem. A* **2020**, *8* (10), 5049−5055.

(9) Yubuchi, S.; Uematsu, M.; Hotehama, C.; Sakuda, A.; Hayashi, A.; Tatsumisago, M. An argyrodite sulfide-based superionic conductor synthesized by a liquid-phase technique with tetrahydrofuran and ethanol. *J. Mater. Chem. A* **2019**, *7* (2), 558−566.

(10) Wenzel, S.; Sedlmaier, S. J.; Dietrich, C.; Zeier, W. G.; Janek, J. Interfacial reactivity and interphase growth of argyrodite solid electrolytes at lithium metal electrodes. *Solid State Ionics* **2018**, *318*, 102−112.

(11) Duchardt, M.; Diels, M.; Roling, B.; Dehnen, S. Flow-Oriented Synthesis of Li2S and Li3PS4·3THF: Opening Up a Completely Solvent-Based Solid Electrolyte Value Chain. *ACS Appl. Energy Mater.* **2020**, *3* (7), 6937−6945.

(12) Li, X.; Zhao, Y.; Brennan, A.; McCeig, M.; Wolden, C. A.; Yang, Y. Reactive Precipitation of Anhydrous Alkali Sulfide Nanocrystals with Concomitant Abatement of Hydrogen Sulfide and Cogeneration of Hydrogen. *ChemSusChem* **2017**, *10* (14), 2904−2913.

(13) Hietala, K.; Zhao, Y.; Yang, Y.; Wolden, C. A. Scalable Synthesis of Alkali Sulfide Nanocrystals Using a Bubble Column Reactor. *Ind. Eng. Chem. Res.* **2018**, *57* (25), 8436−8442.

(14) Zhao, Y.; Yang, Y.; Wolden, C. A. Scalable Synthesis of Size-Controlled Li2S Nanocrystals for Next-Generation Battery Technologies. *ACS Appl. Energy Mater.* **2019**, *2* (3), 2246−2254.

(15) Zhao, Y.; Smith, W.; Wolden, C. A. Scalable synthesis of Li2S nanocrystals for solid-state electrolyte applications. *J. Electrochem. Soc.* **2020**, *167*, 070520.

(16) Yuan, K.; Yuan, L.; Chen, J.; Xiang, J.; Liao, Y.; Li, Z.; Huang, Y. Methods and Cost Estimation for the Synthesis of Nanosized Lithium Sulfide. *Small Struct.* **2021**, *2* (3), 2000059.

(17) Jacob, S. R.; Brown, P. M. Process for producing high-purity lithium sulfide. U. S. Pat.US4126666, 1978.

(18) Yamamoto, K.; Ikeda, N. Method of Manufacturing Lithium Sulfide. Eur. Pat.EP0802159A1, 1997.

(19) Zhang, Y.; Xie, M.-X.; Zhang, W.; Yan, J.-L.; Shao, G.-Q. Synthesis and purification of SiS2 and Li2S for Li9.54-Si1.74P1.44S11.7Cl0.3 solid electrolyte in Lithium-ion batteries. *Mater. Lett.* **2020**, *266*, 127508.

(20) Mohan, G.; Venkataraman, M.; Gomez-Vidal, J.; Coventry, J. Thermo-economic analysis of high-temperature sensible thermal storage with different ternary eutectic alkali and alkaline earth metal chlorides. *Sol. Energy* **2018**, *176*, 350−357.

(21) Liu, X. H.; Yi, X. Q.; Jiang, Y. Mass transfer performance comparison of two commonly used liquid desiccants: LiBr and LiCl aqueous solutions. *Energy Convers. Manage.* **2011**, *52* (1), 180−190.

(22) Smith, W. H.; Birnbaum, J.; Wolden, C. A. Production and purification of anhydrous sodium sulfide. *J. Sulfur Chem.* **2021**, *42* (4), 426−442.
(23) Wang, C.; Wang, X.; Yang, Y.; Kushima, A.; Chen, J.; Huang, Y.; Li, J. Slurryless Li2S/Reduced Graphene Oxide Cathode Paper for High-Performance Lithium Sulfur Battery. *Nano Lett.* **2015**, *15* (3), 1796−1802.
(24) Kim, H.; Jang, H. D.; Choi, M. Facile synthesis of macroporous Li4SiO4 with remarkably enhanced CO2 adsorption kinetics. *Chem. Eng. J.* **2015**, *280*, 132−137.
(25) Rosen, E.; Tegman, R. A preparative and X-ray powder diffraction study of the polysulfides Na2S2, Na2S4 and Na2S5. *Acta Chem. Scand.* **1971**, *25*, 3329−3336.
(26) Deiseroth, H.-J.; Maier, J.; Weichert, K.; Nickel, V.; Kong, S.-T.; Reiner, C. Li7PS6 and Li6PS5X (X: Cl, Br, I): Possible Three-dimensional Diffusion Pathways for Lithium Ions and Temperature Dependence of the Ionic Conductivity by Impedance Measurements. *Z. Anorg. Allg. Chem.* **2011**, *637* (10), 1287−1294.
(27) Randrema, X.; Barcha, C.; Chakir, M.; Viallet, V.; Morcrette, M. A detailed characterisation study of Li6PS5Cl ionic conductors from several synthetic routes. *Solid State Sci.* **2021**, *118*, 106681.
(28) Rao, R. P.; Sharma, N.; Peterson, V. K.; Adams, S. Formation and conductivity studies of lithium argyrodite solid electrolytes using in-situ neutron diffraction. *Solid State Ionics* **2013**, *230*, 72−76.
(29) Yu, C.; Ganapathy, S.; Hageman, J.; van Eijck, L.; van Eck, E. R. H.; Zhang, L.; Schwietert, T.; Basak, S.; Kelder, E. M.; Wagemaker, M. Facile Synthesis toward the Optimal Structure-Conductivity Characteristics of the Argyrodite Li6PS5Cl Solid-State Electrolyte. *ACS Appl. Mater. Interfaces* **2018**, *10* (39), 33296−33306.
(30) Han, F.; Westover, A. S.; Yue, J.; Fan, X.; Wang, F.; Chi, M.; Leonard, D. N.; Dudney, N. J.; Wang, H.; Wang, C. High electronic conductivity as the origin of lithium dendrite formation within solid electrolytes. *Nat. Energy* **2019**, *4* (3), 187−196.
(31) Wang, S.; Zhang, Y.; Zhang, X.; Liu, T.; Lin, Y. H.; Shen, Y.; Li, L.; Nan, C. W. High-Conductivity Argyrodite Li6PS5Cl Solid Electrolytes Prepared via Optimized Sintering Processes for All-Solid-State Lithium-Sulfur Batteries. *ACS Appl. Mater. Interfaces* **2018**, *10* (49), 42279−42285.
(32) Murodjon, S.; Yu, X.; Li, M.; Duo, J.; Deng, T. *Lithium Recovery from Brines Including Seawater, Salt Lake Brine, Underground Water and Geothermal Water*; IntechOpen, 2020. DOI: 10.5772/intechopen.90371.
(33) Guo, Z. Y.; Ji, Z. Y.; Chen, Q. B.; Liu, J.; Zhao, Y. Y.; Li, F.; Liu, Z. Y.; Yuan, J. S. Prefractionation of LiCl from concentrated seawater/salt lake brines by electrodialysis with monovalent selective ion exchange membranes. *J. Clean Prod.* **2018**, *193*, 338−350.
(34) Zhou, L.; Park, K.-H.; Sun, X.; Lalère, F.; Adermann, T.; Hartmann, P.; Nazar, L. F. Solvent-Engineered Design of Argyrodite Li6PS5X (X = Cl, Br, I) Solid Electrolytes with High Ionic Conductivity. *ACS Energy Lett.* **2019**, *4* (1), 265−270.

https://doi.org/10.1021/acsaem.2c00442
ACS Appl. Energy Mater. XXXX, XXX, XXX−XXX